

Electron Microscopy and Neutron Diffraction Studies on $\text{ErBaSrCu}_{3-x}(\text{PO}_4)_x\text{O}_y$ ($x = 0.0, 0.10, 0.20$)

K. N. Marimuthu,* U. V. Varadaraju,*¹ M. Hervieu,† B. Raveau,† S. K. Malik,‡ and W. B. Yelon§

*Materials Science Research Centre, Indian Institute of Technology, Madras-600 036, India; †Laboratoire Crismat, ISMRA-Université de Caen, Boulevard du Maréchal Juin, 14050, Caen Cedex, France; ‡Tata Institute of Fundamental Research, Mumbai 400 005, India; and §University of Missouri Research Reactor Facility, Columbia, Missouri 65211

Received July 12, 1999; in revised form November 8, 1999; accepted November 22, 1999

The structure of a newly stabilized superconducting phase $\text{ErBaSrCu}_{2.9}(\text{PO}_4)_{0.1}\text{O}_y$ was studied by means of electron microscopy and powder neutron diffraction. The electron microscopy study on $\text{ErBaSrCu}_{2.9}(\text{PO}_4)_{0.1}\text{O}_y$ revealed the existence of a tweed-like structure. Rietveld refinement was carried out on $\text{ErBaSrCu}_{3-x}(\text{PO}_4)_x\text{O}_y$ ($x = 0.0, 0.10$, and 0.20) with the orthorhombic space group $Pmmm$. Substitution of the phosphate group at the copper site in $\text{ErBaSrCu}_{3-x}(\text{PO}_4)_x\text{O}_y$ influenced $\text{Cu}(2)\text{-O}$ planes strongly. © 2000 Academic Press

Key Words: oxyanion superconductors; electron diffraction; high-resolution electron microscopy; powder neutron diffraction.

1. INTRODUCTION

The 90 K superconducting compound $\text{YBa}_2\text{Cu}_3\text{O}_7$ is amenable to extensive chemical substitutions at Y, Ba, and Cu sites (1). Substitution at the Y site by a rare earth (RE) ion gives isostructural phases, RE-123 (with a few exceptions), which also exhibit high T_c (except Pr-123). Y-123 does not tolerate any vacancies at the Y site and substitution by an aliovalent ion is possible only to a limited extent, e.g., $(\text{Y}_{1-x}\text{Ca}_x)\text{-123}$. In the latter case, T_c always decreases (1). Substitution of Sr at the Ba site, viz., $\text{YBa}_{2-x}\text{Sr}_x\text{Cu}_3\text{O}_7$ is possible only up to $x = 1.0$, but T_c is always less compared with that of Y-123 (2). The Sr-containing analogues of Y-123, however, can be stabilized under high pressure (3, 4) or by substitution of metal cations like Al, Ga, Pb, Fe, Co, Mn, Mo, W, and Re (5–12) at the chain copper site. More interestingly, substitution of oxyanions like CO_3^{2-} , BO_3^{3-} , SO_4^{2-} , and PO_4^{3-} at the copper site in the basal plane stabilizes $\text{YSr}_2\text{Cu}_3\text{O}_7$ in the 123 structure (13–16). All the oxyanion substituted Sr analogues of Y-123 exhibit semiconducting behavior and superconductivity can be in-

duced by partial substitution of Y^{3+} with a divalent alkaline earth cation like Ca^{2+} or by partial replacement of Sr^{2+} with Ba^{2+} (15–17).

Badri *et al.* (18) reported multiphase formation (211 impurity phase) for phases containing smaller rare earths ($\text{RE} = \text{Er}, \text{Tm}, \text{Yb}, \text{Lu}$) in the $\text{REBaSrCu}_3\text{O}_7$ system and the proportion of the impurity phase increases significantly as the size of RE^{3+} decreases. Marimuthu *et al.* (19) have stabilized $\text{ErBaSrCu}_3\text{O}_{7-\delta}$ in the 123 structure by substituting the phosphate group (PO_4^{3-}) at the copper site. The substitution of the phosphate group at the chain copper site in $\text{ErBaSrCu}_{3-x}(\text{PO}_4)_x\text{O}_y$ ($0.0 \leq x \leq 0.30$) leads to single-phase formation for the compositions $x = 0.10$ and $x = 0.15$ (19). The results of powder X-ray diffraction studies indicate that the single-phase compounds $\text{ErBaSrCu}_{2.9}(\text{PO}_4)_{0.1}\text{O}_y$ and $\text{ErBaSrCu}_{2.85}(\text{PO}_4)_{0.15}\text{O}_y$ crystallize in tetragonal structure and are found to be superconducting with $T_{c, \text{zero}}$ 54 and 37 K, respectively (19). In this paper, we report the results of electron diffraction and high-resolution electron microscopy (HREM) studies on single-phase $\text{ErBaSrCu}_{2.9}(\text{PO}_4)_{0.1}\text{O}_y$. We also report the results of powder neutron diffraction studies on $\text{ErBaSrCu}_{3-x}(\text{PO}_4)_x\text{O}_y$ ($x = 0, 0.1, 0.2$) at room temperature to understand the structure and superconducting properties.

2. EXPERIMENTAL

The compounds in the series $\text{ErBaSrCu}_{3-x}(\text{PO}_4)_x\text{O}_y$ ($0.0 \leq x \leq 0.30$) were prepared by high-temperature solid state reaction method from the respective highly pure oxides, carbonates, and $\text{NH}_4\text{H}_2\text{PO}_4$. The detailed method of preparation has been described elsewhere (19). Phase purity was confirmed by powder X-ray diffraction ($\text{CuK}\alpha_1$ radiation). The oxygen content was estimated by the iodometry method. The samples for electron microscopy were prepared by grinding the powder in alcohol. Small crystallites in suspension were deposited on a carbon film, supported by a nickel grid. The electron diffraction (ED) study was

¹To whom correspondence should be addressed. Fax: +91 044 2350509. E-mail: raju@msrc.iitm.ernet.in.

carried out using a JEOL 200 CX electron microscope fitted with an eucentric goniometer ($\pm 60^\circ$) and equipped with an EDX analyzer. HREM was performed with a TOPCON 002B operating at 200 kV (point resolution of 1.8 Å). Neutron diffraction data were collected at the University of Missouri Research Reactor using the high-resolution linear position-sensitive detector diffractometer. The neutron wavelength was 1.7675 Å. Approximately 2 g of finely powdered sample was contained in a thin-walled vanadium holder. Data were collected at room temperature with 2θ values 5° to 105° in 0.05° steps. Refinement of the neutron diffraction data was carried out by the Rietveld method using the FULLPROF program, which permits multiple phase refinement as well as magnetic structure refinement (20). The structural parameters of YSr₂Cu_{2.78}(SO₄)_{0.22}O_{6.21} were used as a starting model for the refinement (15). The positional, thermal (B), and occupancy parameters were varied in addition to scale factor, zero angle, and half-width and background parameters. The occupancy and thermal parameters were varied in separate cycles.

3. RESULTS AND DISCUSSION

3.1. ED and HREM Studies on Single-Phase

ErBaSrCu_{2.9}(PO₄)_{0.1}O_y

EDX analysis of single-phase ErBaSrCu_{2.9}(PO₄)_{0.1}O_y was performed on numerous crystallites. The analysis clearly showed that the cation ratio Er/Ba/Sr is very close to 1/1/1, which is in agreement with the nominal composition, and the copper content is also close to 2.9. The analysis also confirmed the presence of phosphorus in each of the investi-

gated crystallites, but the exact phosphorus content could not be determined accurately due to the low content which is close to the limit of accuracy of the technique. The reconstruction of the reciprocal space was performed by tilting about the three crystallographic axes and the [110]* direction. Figure 1 shows the typical [100] ED pattern of the ErBaSrCu_{2.9}(PO₄)_{0.1}O_y phase. The system of intense Bragg dots confirmed that the compound exhibits a 123-type structure with $a \approx b \approx a_p \approx 3.84$ Å and $c \approx 3a_p \approx 11.5$ Å (a_p is the parameter of the ideal cubic perovskite cell). The lattice parameter values are in agreement with values obtained from powder X-ray diffraction ($a = b = 3.831$ Å and $c = 11.507$ Å) (19).

Two types of twinning phenomena are systematically observed in the electron diffraction investigation of the phosphate-substituted single-phase ErBaSrCu_{2.9}(PO₄)_{0.1}O_y. First, the 123-mode oxygen ordering is found along one of the three equivalent [100]_p directions of the cubic perovskite subcell. This is illustrated in Fig. 2. The electron diffraction pattern in Fig. 2a shows the superposition of [001] and [100] variants. The corresponding brightfield image (Fig. 2b) clearly shows a [100] domain (54 nm wide) which exhibits coherent boundaries with the [001] matrix. The boundaries are parallel to the (100)_p planes of the perovskite subcell. A second feature deals with the cross shape of the $hk0$ Bragg spots, which is evident only for high h and k values. The arms of the crosses are extended along the [110]* and $[\bar{1}\bar{1}0]^*$ directions. This can be considered as a signature of a very low orthorhombicity of the structure, similar to that observed in Fe-doped YBa₂Cu₃O₇ (21, 22). The low orthorhombicity results in the formation of small domains, of the two [100] and [010] variants, so that the crystallites exhibit a weak contrast characteristic of a “tweedlike” structure (see [100] domain in Fig. 2b).

High-resolution images were recorded along the [100] or [010] zone. The images are very similar to those usually observed for 123-type materials. Figure 3 presents the typical HREM image of the ErBaSrCu_{2.9}(PO₄)_{0.1}O_y phase in which the [Cu₍₁₎O]_∞ layers appears rows of brighter dots. One observes that the brightness of the dots is more or less intense along one row. Such a variation in contrast is not observed in the LnBa₂Cu₃O₇ system, but is systematically observed in 123-oxycarbonates (13, 24, 27). By analogy, this variation in contrast is attributed to the presence of phosphate groups in the structure. It is also observed that there is no regular spacing between dots of equal brightness. This shows that there is no ordering between the Cu(I)O₄ square planar groups and the phosphate (PO₄³⁻) groups. This observation is in agreement with [100] ED patterns where no extra reflections were observed. This is in contrast to what is observed in the 123-oxycarbonates and oxysulfates (13, 24–27), where superstructure spots, sometimes intense, are systematically present.

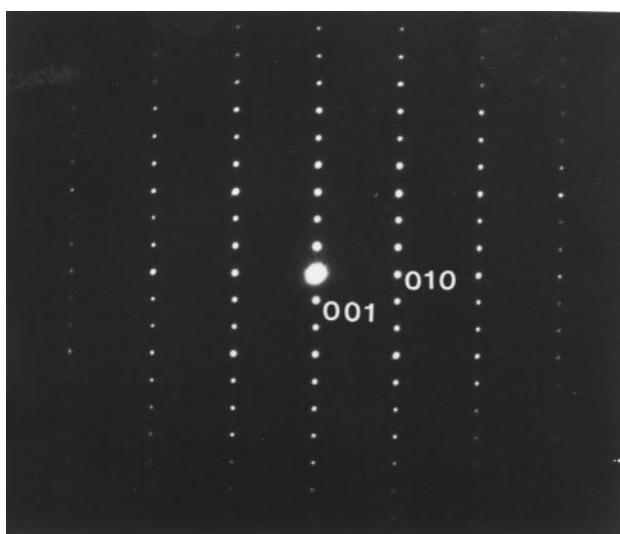


FIG. 1. Electron diffraction pattern of ErBaSrCu_{2.9}(PO₄)_{0.1}O_y along [100].

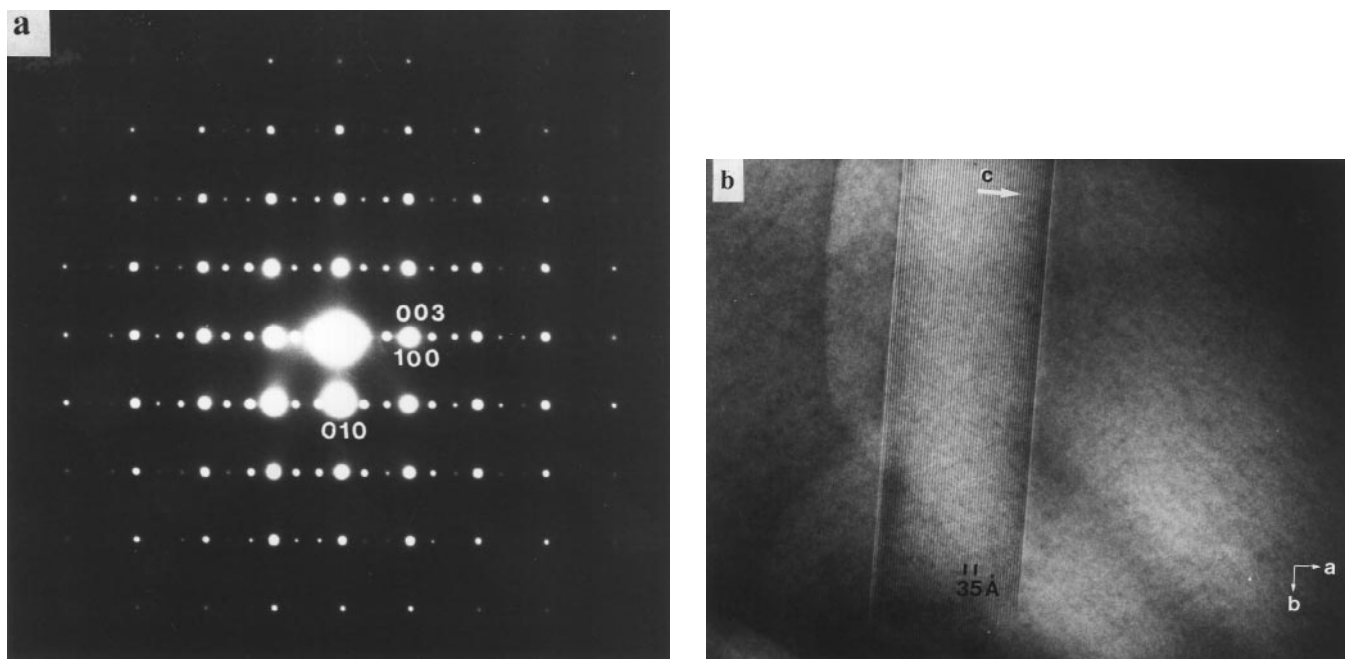


FIG. 2. (a) Electron diffraction pattern of $\text{ErBaSrCu}_{2.9}(\text{PO}_4)_{0.1}\text{O}_y$ as a superposition of [001] and [100] variants. (b) Corresponding brightfield image showing [100] domain.

3.2. Powder Neutron Diffraction Studies on $\text{ErBaSrCu}_{3-x}(\text{PO}_4)_x\text{O}_y$ ($x = 0, 0.10, 0.20$)

3.2.1. Powder neutron diffraction study on $\text{ErBaSrCu}_3\text{O}_y$. The nominal composition $\text{ErBaSrCu}_3\text{O}_y$ results in multiphase formation with the 123 phase as the major component (19). The refinement for the predominant 123 phase ($\text{ErBaSrCu}_3\text{O}_y$) was carried out using the orthorhombic space group $Pmmm$ with the coordinates of the 123 structure

as the starting set of parameters. At the initial stage, all structural parameters were kept constant and instrumental parameters were refined. The structural parameters were then refined independently. The isotropic temperature factors (B) and occupancy factors were not allowed to vary simultaneously because of their strong correlation. To determine the oxygen occupancy ordering, the O(1) and O(5) oxygen occupancies were allowed to vary simultaneously. Ba and Sr were assumed to be randomly distributed in $2t$

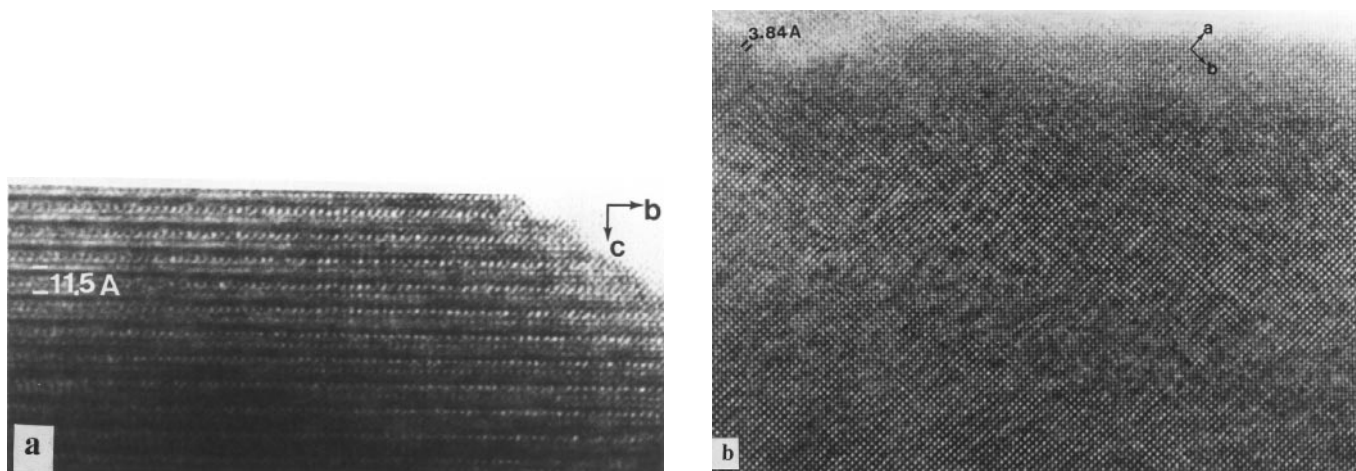


FIG. 3. High-resolution images of $\text{ErBaSrCu}_{2.9}(\text{PO}_4)_{0.1}\text{O}_y$ taken with the incident beams parallel to (a) [100] and (b) [001].

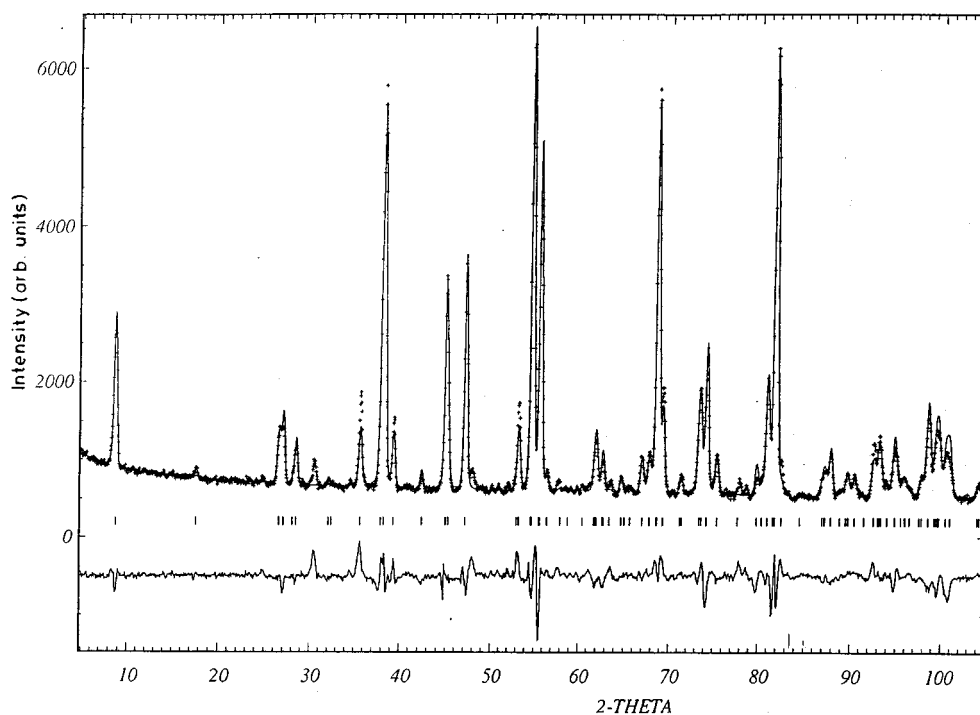


FIG. 4. Rietveld refinement profile for the multiphase ErBaSrCu₃O_y (refinement was carried out for the predominant 123 phase, i.e., ErBaSrCu₃O_y in orthorhombic space group *Pmmm*). The plus signs represent the raw neutron powder diffraction data. The solid line is the calculated profile. Tick marks below the diffraction profile mark the positions of allowed Bragg reflections. A difference curve (observed minus calculated) is plotted at the bottom.

sites as in YBaSrCu₃O₇ (23). Figure 4 shows the observed (crosses) and calculated (solid line) neutron diffraction patterns along with the difference curve. The lattice constants obtained from the refinement for the predominant 123 phase ErBaSrCu₃O_y are $a = 3.7917(1) \text{ \AA}$, $b = 3.8506(2) \text{ \AA}$, and $c = 11.5730(8) \text{ \AA}$. The reliability factors are found to be $R_p = 5.05$, $WR_p = 6.97$, and Bragg R factor = 6.26. The occupancy factors of the O(1) and O(5) sites are 0.89(2) and 0.12(2), respectively. The occupation at the O(5) site (1b site) merely indicates disorder in the existing orthorhombic structure. The Cu–O distances [Cu(2)–O(2) = 1.913(1) Å; Cu(2)–O(3) = 1.942(1) Å; Cu(2)–O(4) = 2.230(6) Å] are, in general, slightly shorter than those observed in ErBa₂Cu₃O₇. This is probably due to the lattice contraction that arises from the substitution of smaller Sr ions for Ba ions. The total oxygen content (7.01) from powder neutron diffraction is higher than the value obtained from chemical analysis (6.78, from iodometry titration).

3.2.2. Powder neutron diffraction study on ErBaSrCu_{2.9}(PO₄)_{0.1}O_y. The structure of single-phase ErBaSrCu_{2.9}(PO₄)_{0.1}O_y was refined on the basis of an orthorhombic unit cell with the space group *Pmmm*. The structural parameters corresponding to YSr₂Cu_{2.78}(SO₄)_{0.22}O_{6.21} were used as the starting values for the refinement (15). Ba and Sr

were assumed to be randomly situated in $2t$ sites as in YBaSrCu₃O₇ (23). To determine the oxygen ordering, the O(1) and O(5) oxygen occupancies were allowed to vary simultaneously. Inclusion of oxygen atoms corresponding to the phosphate group into the final refinement and use of sensible constraints on site occupancies and temperature factors produced a satisfactory fit. Figure 5 shows the observed (crosses) and calculated (solid line) neutron diffraction patterns along with the difference curve. Tables 1 and 2 list the final structural parameters and interatomic distances. The refined Cu(1) occupancy is consistent with complete occupancy of the chain sites by Cu and P. The lower occupancy at O(1) and significant occupation at O(5) site [0.38(2)] with high thermal factors (B) merely indicate the presence of disorder in the existing orthorhombic structure. During the refinement, similar to sulfate-substituted YSr₂Cu₃O₇ (15), the occupancy for O(4) was fixed at twice that of Cu(1) as incorporation of each phosphate group into YBaSrCu₃O₇ structure leads to elimination of two O(4) atoms. The refined lattice constants are $a = 3.8313(2) \text{ \AA}$, $b = 3.8373(2) \text{ \AA}$, and $c = 11.5275(5) \text{ \AA}$. It is evident that the degree of orthorhombicity, $(b - a)/a$, is very small (0.16). The contraction in the c -axis is due to elimination (or displacement) of the apical oxygen O(4). The total oxygen content [7.01 (including the oxygen content in the

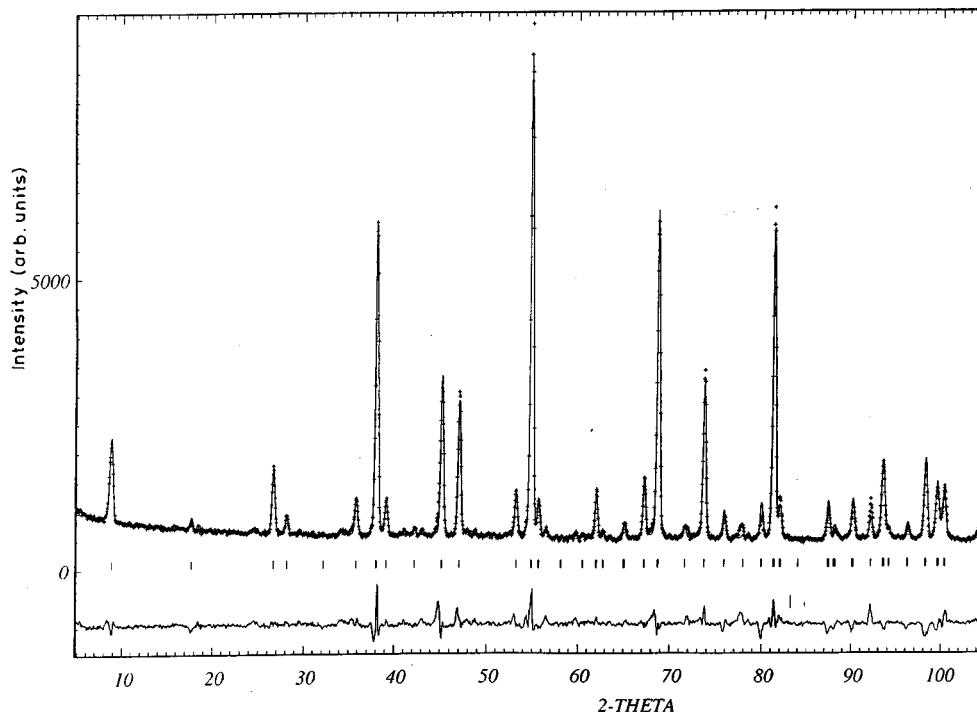


FIG. 5. Rietveld refinement profile for orthorhombic (space group $Pmmm$) $\text{ErBaSrCu}_{2.9}(\text{PO}_4)_{0.1}\text{O}_{6.61}$. The plus signs represent the raw neutron powder diffraction data. The solid line is the calculated profile. Tick marks below the diffraction profile mark the positions of allowed Bragg reflections. A difference curve (observed minus calculated) is plotted at the bottom.

phosphate group)] obtained from powder neutron diffraction is in agreement with the analytical value 6.97, determined from iodometry titration. Figure 6 shows the

structure of $\text{ErBaSrCu}_{2.9}(\text{PO}_4)_{0.1}\text{O}_y$ (present study) along with that of $\text{YBa}_2\text{Cu}_3\text{O}_7$. Incorporation of each phosphate group into the $\text{ErBaSrCu}_3\text{O}_7$ structure eliminates two O(4) atoms (apical oxygen atoms), which normally link the superconducting CuO_2 layer with the Cu(1) sites, and displaces the Sr and Ba atoms from the normal $2t$ site to a half-occupied $4x$ site. As a result of this, the copper in $\text{Cu}(2)\text{O}_2$ planes can have both fourfold (square planar) and fivefold

TABLE 1
Structural Parameters for $\text{ErBaSrCu}_{2.9}(\text{PO}_4)_{0.1}\text{O}_y$ Deduced by the Rietveld Refinement of Neutron Diffraction Data

Atom	Wyckoff symbol	x	y	z	B (Å)	Unit cell occupancy
Er	1h	0.5	0.5	0.5	0.2(1)	1
Ba	4x	0.455(4)	0	0.1851(4)	1.1(1)	1
Sr	4x	0.455(4)	0	0.1851(4)	1.1(1)	1
Cu(1)	1a	0	0	0	2.2(1)	0.90(4)
P	1a	0	0	0	2.2(1)	0.1
Cu(2)	2q	0	0	0.3561(3)	0.83(6)	2
O(1)	1e	0	0.5	0	3.6(6)	0.43(2)
O(2)	2s	0.5	0	0.3882(6)	1.0(1)	2
O(3)	2r	0	0.5	0.3683(5)	0.7(1)	2
O(4)	2q	0	0	0.1629(5)	1.0(1)	1.8
O(5)	1b	0	0	0	3.6(6)	0.38(2)
O(6)	4w	0.22(2)	0	0.114(7)	1.00	0.20
O(7)	4y	0.24(2)	0.34(1)	0	1.00	0.20

Note. Space group: $Pmmm$: $a = 3.8313(2)$ Å, $b = 3.8373(2)$ Å, and $c = 11.5275(5)$ Å. $R_p = 4.30$, $R_{wp} = 5.76$, $R_{exp} = 3.44$, $\chi^2 = 2.80$ and Bragg R factor = 6.16.

Constraints: The temperature factors for O(6) and O(7) were held equal. The unit cell occupancies of Er, Ba, Sr, and PO_4 were weighed out. The occupancy for O(4) was fixed at twice that of Cu(1).

TABLE 2
Selected Bond Distances (Å) and Bond Angles (°) for $\text{ErBaSrCu}_{2.9}(\text{PO}_4)_{0.1}\text{O}_y$

Bond distances (Å)			
Cu(1)–O(1)	$1.9190(1) \times 2$	Er–O(2)	$2.312(4) \times 4$
Cu(1)–O(4)	$1.879(6) \times 2$	Er–O(3)	$2.445(3) \times 4$
Cu(2)–O(2)	$1.951(1) \times 2$	Ba–O(2)	$3.031(7) \times 2$
Cu(2)–O(3)	$1.9240(5) \times 2$	Ba–O(3)	$2.74(1) \times 2$
Cu(2)–O(4)	$2.226(7) \times 1$		
P–O(6)	$1.57(8) \times 2$		
P–O(7)	$1.63(7) \times 2$		
Bond angles (°)			
Cu(2)–O(2)–Cu(2)	158.1(3)		
Cu(2)–O(3)–Cu(2)	171.6(2)		
O(7)–P–O(7)	109(4)		
O(6)–P–O(6)	114(4)		
O(7)–P–O(6)	108(2)		

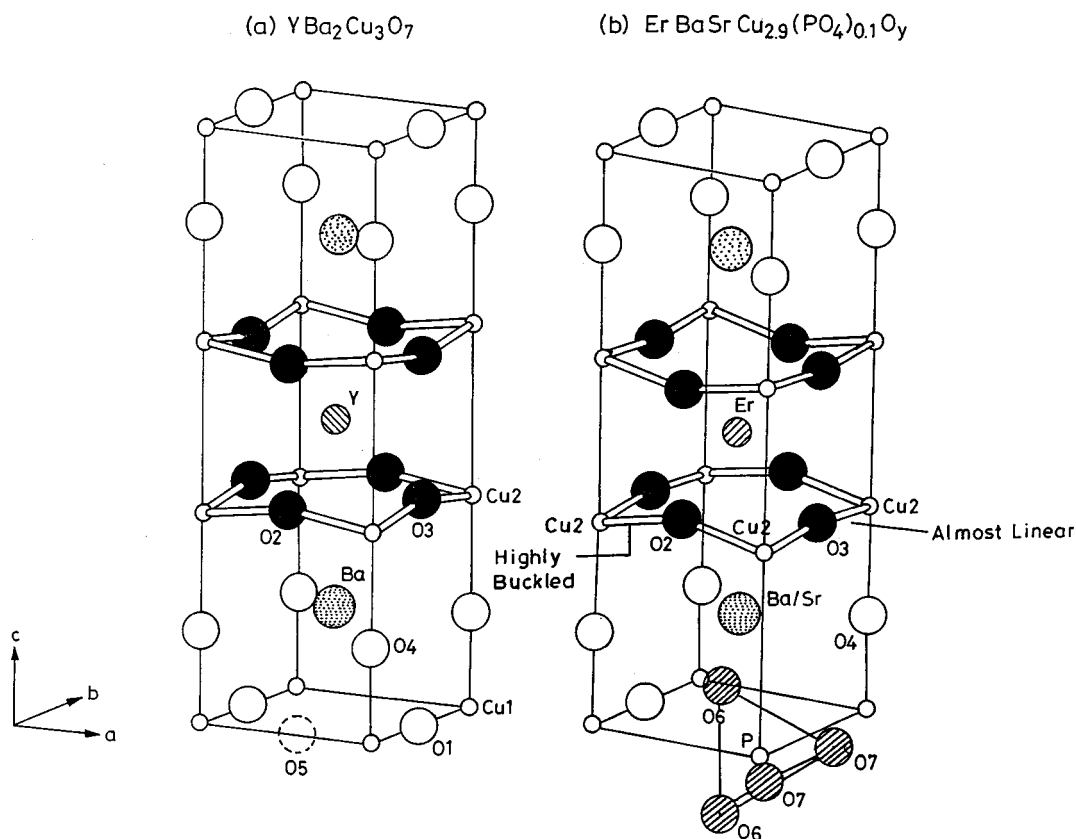


FIG. 6. Structures of (a) $\text{YBa}_2\text{Cu}_3\text{O}_7$ [drawn from the coordinates given in Jorgensen *et al.* (35)] and (b) phosphate-incorporated single-phase $\text{ErBaSrCu}_{2.9}(\text{PO}_4)_{0.1}\text{O}_y$ showing highly buckled $\text{Cu}(2)\text{-O}(2)\text{-Cu}(2)$ and highly flat (almost linear) $\text{Cu}(2)\text{-O}(3)\text{-Cu}(2)$ planes.

(square pyramidal) coordination as observed in $\text{YSr}_2\text{Cu}_{2.78}(\text{SO}_4)_{0.22}\text{O}_{6.21}$ by Slater *et al.* (15). In fact, the O(6) atoms may be regarded as O(4) atoms that have been displaced to form P–O bonds. The substitution of a phosphate group at the chain copper site influences the CuO_2 planes strongly. This is due to the elimination of O(4) atoms and the displacement of Sr and Ba atoms from the normal $2t$ site. The $\text{Cu}(2)\text{-O}(2)\text{-Cu}(2)$ and $\text{Cu}(2)\text{-O}(3)\text{-Cu}(2)$ bond angles are 158° and 171° , respectively (Table 2). This is in contrast to the $\text{YBa}_2\text{Cu}_3\text{O}_7$ system in which the in-plane Cu–O–Cu bond angles are almost equal (164°). Thus, it is interesting to note that in phosphate-substituted $\text{ErBaSrCu}_3\text{O}_7$, the CuO_2 planes have both highly flat (almost linear) Cu–O(3)–Cu planes and highly buckled Cu–O(2)–Cu planes. The corresponding Cu(2)–O(2) and Cu(2)–O(3) bond distances are 1.951(1) and 1.924(0) Å, respectively. The observed Cu(2)–O bond distances in $\text{ErBaSrCu}_{2.9}(\text{PO}_4)_{0.1}\text{O}_y$ are different from those in $\text{YBa}_2\text{Cu}_3\text{O}_7$ [Cu(2)–O(2) and Cu(2)–O(3) bond distances in $\text{YBa}_2\text{Cu}_3\text{O}_7$ are 1.929 and 1.958 Å, respectively] (28). The P–O(6) and P–O(7) bond distances are 1.57(8) and 1.63(7) Å, respectively. The P–O bond angles are close to tetrahedral bond angles (Table 2) and the orientation of distorted PO_4

tetrahedra is shown in Fig. 6. The decrease in $T_{c, \text{zero}}$ (54 K) for the phosphate-substituted $\text{ErBaSrCu}_{2.9}(\text{PO}_4)_{0.1}\text{O}_y$ could be attributed to the observed lower copper valence and the displacements of both the in-plane and bridging oxygens as compared with 90 K superconducting $\text{ErBa}_2\text{Cu}_3\text{O}_{7-\delta}$.

3.2.3. *Bond valence sum (bond strength sum) of copper in $\text{ErBaSrCu}_{2.9}(\text{PO}_4)_{0.1}\text{O}_y$.* The bond valence sum of copper in $\text{ErBaSrCu}_{2.9}(\text{PO}_4)_{0.1}\text{O}_y$ was calculated using the equation (29–31).

$$V_j = \sum_j S_{ij} = \sum_j \exp(R_0 - R_{ij}/B), \quad [1]$$

where $R_0 = 1.679$ Å for Cu^{2+} , $B = 0.37$ Å [values are taken from Ref. (30)] and R_{ij} = respective Cu–O bond distances [from in-plane and apical oxygens in the square pyramidal geometry Cu(2) only].

The calculated $V_{\text{Cu in-plane}}$, $V_{\text{Cu out-of-plane}}$, and total bond valence sum of copper V_{Cu} were 1.9902, 0.2280, and 2.2182, respectively. In the present study, only the bond valence sum of Cu(2) is calculated and the value is compared with

bond valence sums of Cu(2) of some cuprates. De Leeuw *et al.* (32) correlated the bond valence sums of copper with T_c for a number of p -type high- T_c cuprates and the authors found that T_c increases with a decrease in bond valence sums. As compared with $\text{YBa}_2\text{Cu}_3\text{O}_7$ ($V_{\text{Cu}} = 2.15$) (34), the bond valence sum of copper in $\text{ErBaSrCu}_{2.9}(\text{PO}_4)_{0.1}\text{O}_y$ is slightly higher and hence T_c is low. This could be explained as due to the difference in the Cu–O bond lengths which arises as a result of the partial replacement of Ba by Sr and substitution of phosphate at the chain copper site. Since the bond valence sum of copper in $\text{ErBaSrCu}_{2.9}(\text{PO}_4)_{0.1}\text{O}_y$ is less than that in $\text{YBaSrCu}_3\text{O}_7$ ($V_{\text{Cu}} = 2.25$) (23), $\text{ErBaSrCu}_{2.9}(\text{PO}_4)_{0.1}\text{O}_y$ should have a higher T_c than $\text{YBaSrCu}_3\text{O}_7$. But experimentally $\text{ErBaSrCu}_{2.9}(\text{PO}_4)_{0.1}\text{O}_y$ has a lower T_c (54 K) than $\text{YBaSrCu}_3\text{O}_7$ (~ 80 K) (2, 12, 18, 23, 33).

The incorporation of a phosphate group (PO_4^{3-}) into $\text{ErBaSrCu}_3\text{O}_7$ eliminates the bridging oxygens (apical oxygens) which normally link the superconducting CuO_2 layers with the Cu(1) sites in the structure. As a result, the charge transfer from the chain to the plane is not effective and hence the superconducting transition temperature of $\text{ErBaSrCu}_{2.9}(\text{PO}_4)_{0.1}\text{O}_y$ is lower than that of $\text{YBaSrCu}_3\text{O}_7$.

3.2.4. Powder neutron diffraction study on $\text{ErBaSrCu}_{2.8}(\text{PO}_4)_{0.2}\text{O}_y$. Even though $\text{ErBaSrCu}_{2.8}(\text{PO}_4)_{0.2}\text{O}_y$ is

multiphasic (minor impurity peaks in XRD) (19), the structure of the predominant 123 phase is refined to understand the effect of increasing phosphate content at the chain copper site on CuO_2 planes. The structure was refined in orthorhombic space group $Pmmm$.

Figure 7 shows the observed (crosses) and calculated (solid line) neutron diffraction patterns along with the difference curve. The refined Cu(1) occupancy is consistent with the complete occupancy of the chain sites by Cu and P. During the refinement, similar to $\text{ErBaSrCu}_{2.9}(\text{PO}_4)_{0.1}\text{O}_y$, the occupancy for O(4) was fixed at twice that of Cu(1). The refined lattice constants are $a = 3.837(4)$ Å, $b = 3.8403(2)$ Å, and $c = 11.5027(6)$ Å. The c axis has further decreased with a slight increase in the a axis as compared with the phosphate-substituted phase with $x = 0.1$. The total oxygen content (7.13) from powder neutron diffraction is in acceptable agreement with the analytical value (7.08). The reliability factors are found to be $R_p = 5.10$, $wR_p = 7.01$, and Bragg R factor = 9.18.

The increase in phosphate content (from 0.1 to 0.2) at the chain copper site does not affect the CuO_2 planes further. The Cu(2)–O(2)–Cu(2) and Cu(2)–O(3)–Cu(2) bond angles are 159° and 173° , respectively. The corresponding Cu(2)–O(2) and Cu(2)–O(3) bond distances are 1.952(2) and 1.923(6) Å, respectively. The O(6)–P–O(6) and O(7)–P–O(7) bond angles are 113° and 123° , respectively. Since the P–O bond angles deviate more from the regular

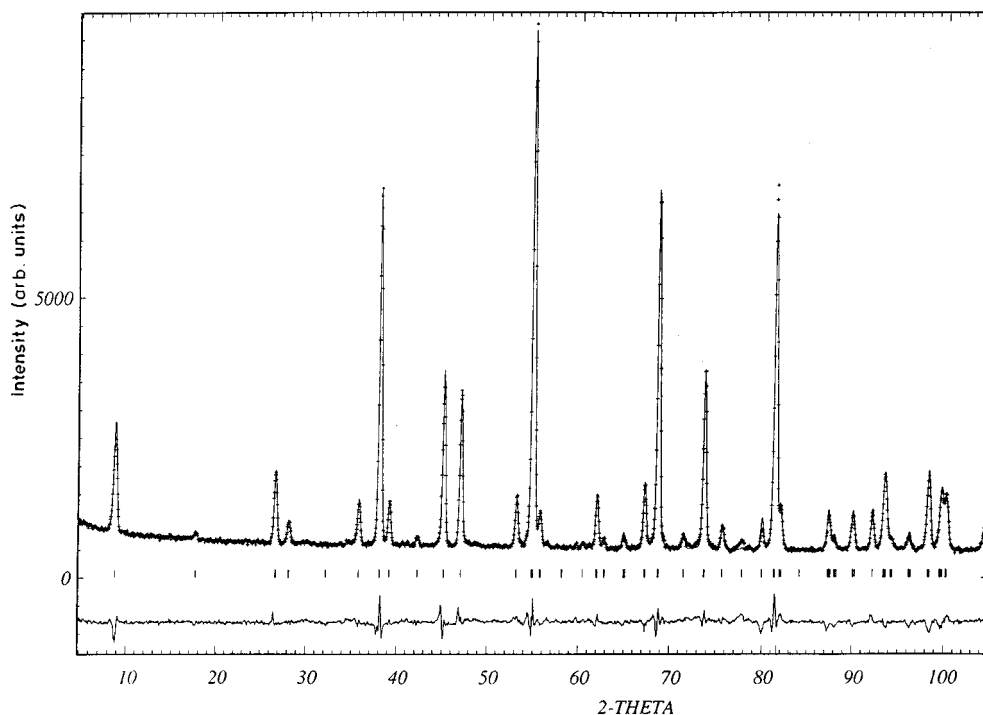


FIG. 7. Rietveld refinement profile for orthorhombic (space group $Pmmm$) $\text{ErBaSrCu}_{2.8}(\text{PO}_4)_{0.2}\text{O}_y$.

tetrahedral bond angle (109° , $28'$), the PO₄ tetrahedra are highly distorted. It is also clear that the orthorhombicity for $x = 0.2$ (0.08) is very low in the series ErBaSrCu_{3-x}(PO₄)_xO_y, indicating that the structure of ErBaSrCu_{2.8}(PO₄)_{0.2}O_y tends more toward tetragonal symmetry.

4. SUMMARY AND CONCLUSIONS

Electron microscopy and neutron diffraction studies confirm the stabilization of a new superconducting copper oxide ErBaSrCu_{2.9}(PO₄)_{0.1}O_y in a 123-type structure. The electron diffraction investigation shows that there is no superstructure reflections in most of the crystallites, and the high-resolution images confirm that this feature occurs randomly. The crystallites are characterized by the formation of two types of twinning domains, with [110] and [001] boundaries, respectively. The first type of twinning domain results from the low orthorhombicity of the cell ($a/b \approx 1$) and the second is due to the peculiar c parameter with $c \approx 3a \approx 3b$, possibly favored by the existence of the phosphate group. Powder neutron diffraction shows that substitution of phosphate at the copper site in ErBaSrCu₃O₇ influences Cu(2)–O planes strongly and the observed Cu(2)–O bond distances are different from those in YBa₂Cu₃O₇. An important feature of this new phosphate-incorporated compound is that the copper in Cu(2)O₂ sheets can exist in both square planar (as in Nd₂CuO₄) and square pyramidal (as in YBa₂Cu₃O_{7- δ}) coordination. The lower formal valence of copper, higher bond valence sum of copper, displacements of both in-plane and bridging oxygens, and ineffective charge transfer from the chain to the Cu(2)O₂ plane could be the reason for the reduction in $T_{c,zero}$ for single-phase ErBaSrCu_{2.9}(PO₄)_{0.1}O_y as compared with ErBa₂Cu₃O_{7- δ} .

ACKNOWLEDGMENTS

The authors thank the referees for critical reading of the manuscript and useful suggestions. One of the authors (K.N.M.) thanks IIT, Madras, for the award of a Senior Research Fellowship.

REFERENCES

- G. V. Subba Rao and U. V. Varadaraju, in "Chemistry of High Temperature Superconductors" (C. N. R. Rao, Ed.), World Scientific, Singapore, 1991.
- B. W. Veal, W. K. Kwok, A. Umezawa, G. W. Crabtree, J. D. Jorgensen, J. W. Downey, L. J. Nowicki, A. W. Mitchell, A. P. Paulikas, and C. H. Sowers, *Appl. Phys. Lett.* **51**, 279 (1987).
- B. Okai, *Jpn. J. Appl. Phys.* **29**, L2180 (1990).
- A. Ono, *Physica C* **198**, 287 (1992).
- S. A. Sunshine, L. F. Schneemeyer, T. Siegrist, D. C. Douglass, J. V. Waszczak, R. J. Cava, E. M. Gyorgy, and D. W. Murphy, *Chem. Mater.* **1**, 331 (1989).
- G. Roth, P. Adelmann, G. Heger, R. Knitter, and Th. Wolf, *J. Phys. I* **1**, 721 (1991).
- T. Den and Kobayashi, *Physica C* **196**, 141 (1992).
- P. R. Slater and C. Greaves, *Physica C* **180**, 299 (1991).
- R. Suryanarayanan and E. Chavira, *Phys. Status. Solidi B* **187**, K67 (1995).
- M. Murugesan, M. S. Ramachandra Rao, L. C. Gupta, R. Pinto, M. Sharon, and R. Vijayaraghavan, *Phys. Rev. B* **53**, 8604 (1996).
- M. Murugesan, P. Selvam, M. Sharon, M. S. R. Rao, L. C. Gupta, R. Pinto, C. S. Gopinath, and S. Subramanian, *Appl. Phys. Lett.* **67**, 2711 (1995).
- R. Suryanarayanan, M. S. R. Rao, L. Ouhammou, O. Gorochoy, N. Le Nagard, and H. Pankowska, *Mater. Sci. Forum* **130–132**, 465 (1993).
- Y. Miyazaki, H. Yamane, N. Ohnishi, T. Kajitani, Y. Morii, S. Funahashi, and T. Hirai, *Physica C* **198**, 7 (1992).
- J. P. Chapman and J. P. Attfield, *Physica C* **235–240**, 351 (1994).
- P. R. Slater, C. Greaves, M. Slaski, and C. M. Muirhead, *Physica C* **208**, 193 (1993).
- R. Nagarajan, S. Ayyapan, and C. N. R. Rao, *Physica C* **220**, 373 (1994).
- J. Akimitsu, M. Uehara, M. Ogawa, H. Nakata, K. Tomimoto, Y. Miyazaki, H. Yamane, T. Hirai, K. Kinoshita, and Y. Matsui, *Physica C* **201**, 320 (1992).
- V. Badri, U. V. Varadaraju, and G. V. Subba Rao, in "Physical and Materials Properties of High Temperature Superconductors" (S. K. Malik and S. S. Shah, Eds.), p. 35. Nova Sci. Publ., New York, 1994.
- K. N. Marimuthu, M. S. Ramachandra Rao, and U. V. Varadaraju, *Physica C* **280**, 327 (1997).
- H. M. Rietveld, *J. Appl. Crystallogr.* **2**, 65 (1969).
- G. Roth, G. Heger, B. Renker, J. Pannetier, V. Caignaert, M. Hervieu, and B. Raveau, *Z. Phys. B* **71**, 43 (1988).
- T. Krekels, G. Van Tendeloo, D. Broddin, S. Amelinckx, L. Tanner, M. Mehdod, E. Vanlathem, and R. Deltour, *Physica C* **173**, 361 (1991).
- Y. Takeda, R. Kanno, O. Tamamoto, M. Takano, Z. Hiroi, Y. Bando, M. Shimada, H. Akinaga, and K. Takita, *Physica C* **157**, 358 (1989).
- B. Domengès, M. Hervieu, and B. Raveau, *Physica C* **207**, 65 (1993).
- T. Krekels, O. Milat, G. Van Tendeloo, J. Van Landuyt, S. Amelinckx, P. R. Slater, and C. Greaves, *Physica C* **210**, 439 (1993).
- G. Van Tendeloo and T. Krekels, *J. Eur. Ceram. Soc.* **16**, 367 (1996).
- I. Monot, K. Verbist, M. Hervieu, P. Laffez, M. P. Delamare, J. Wang, G. Desgardin, and G. Van Tendeloo, *Physica C* **274**, 253 (1997).
- W. I. F. David, W. T. A. Harrison, J. M. F. Gunn, O. Moze, A. K. Soper, P. Day, J. D. Jorgensen, D. G. Hinks, M. A. Beno, L. Soderholm, D. W. Capone II, I. K. Schuller, C. U. Segre, K. Zhang, and J. D. Grace, *Nature* **327**, 310 (1987).
- W. H. Zachariassen, *J. Less-Common Met.* **62**, 1 (1978).
- I. D. Brown and D. Altermatt, *Acta Crystallogr. B* **41**, 244 (1985).
- I. D. Brown and R. D. Shannon, *Acta Crystallogr. A* **29**, 266 (1973).
- D. M. de Leeuw, W. A. Groen, L. F. Feiner, and E. E. Havinga, *Physica C* **166**, 133 (1990).
- V. Badri, Ph.D. thesis IIT, Madras, 1995.
- M. Francois, A. Junod, K. Yvon, A. W. Hewat, and P. Fischer, *Solid State Commun.* **66**, 1117 (1988).
- J. D. Jorgensen, B. W. Veal, A. P. Paulikas, L. J. Nowicki, G. W. Crabtree, H. Claus, and W. K. Kwok, *Phys. Rev. B* **41**, 1863 (1990).